



Get Clarity On Generics

Cost-Effective CT & MRI Contrast Agents



FRESENIUS
KABI

WATCH VIDEO

AJNR

MR Imaging of Paragangliomas

Walter L. Olsen, William P. Dillon, William M. Kelly, David Norman, Michael Brant-Zawadzki and T. Hans Newton

AJNR Am J Neuroradiol 1986, 7 (6) 1039-1042
<http://www.ajnr.org/content/7/6/1039>

This information is current as
of August 11, 2025.

MR Imaging of Paragangliomas

Walter L. Olsen¹
 William P. Dillon
 William M. Kelly
 David Norman
 Michael Brant-Zawadzki
 T. Hans Newton

MR imaging of 15 paragangliomas in 10 patients was compared with CT of 13 of the lesions in eight patients. All lesions were confirmed with angiography. All lesions were detected by MR and CT with the exception of one small glomus tympanicum tumor that was seen only in retrospect with MR. CT better demonstrated subtle osseous changes of the skull base and the relation of the tumor to the middle ear structures. MR better demonstrated the relation of the tumor to the adjacent internal jugular vein and carotid artery. The paragangliomas had a characteristic MR appearance based on their vascularity. Serpiginous areas of signal void representing high vascular flow were interspersed among areas of high signal intensity caused by slowly flowing blood and tumor cells. This "salt-and-pepper" pattern was seen in all lesions greater than 2 cm in maximal dimension. MR was therefore able to accurately characterize the tumors as highly vascular. Multiplanar imaging and good tissue contrast and anatomic detail permitted display of the relations of these neoplasms to surrounding carotid sheath vessels and to intracranial structures better than did CT. In this experience, the MR appearance of paragangliomas was quite characteristic and differed markedly from meningiomas, neuromas, and metastatic disease of the skull base.

Paragangliomas are slowly growing hypervascular tumors arising from neural crest cell derivatives throughout the body. In the head and neck region, the major paraganglial cells are located at the carotid bifurcation (carotid body), along the nodose ganglia of the vagus nerve, and along the nerves supplying the middle ear and jugular bulb. In recent years, CT and angiography have been the primary radiologic tools used to investigate the paragangliomas. Contrast-enhanced CT studies demonstrate an enhancing mass either at the carotid bifurcation or in the region of the jugular foramen. The vascular nature of paragangliomas can be detected by dynamic CT scanning during a rapid bolus of intravenous contrast material [1-3] or by angiography, which demonstrates the typical hypervascular mass supplied by the external carotid artery. Bolus dynamic CT scanning has not gained wide acceptance, as this technique involves a second rapid infusion of contrast material after the initial diagnostic study. Angiography demonstrates the highly vascular nature of the tumor and permits either palliative or preoperative embolization, if appropriate.

The role of MR imaging in the evaluation of patients with paragangliomas has not been established. Therefore, we reviewed retrospectively 15 proven examples of paragangliomas of the head and neck imaged with MR, angiography, and, in most cases, CT. The ability of MR to identify the nature and extent of paragangliomas and their relation to adjacent structures was assessed.

Materials and Methods

Ten patients with 15 paragangliomas were studied with MR imaging. One patient had bilateral carotid body tumors. Two patients had a carotid body tumor on one side and a contralateral glomus jugulare tumor. One patient had bilateral carotid body tumors with a

This article appears in the November/December 1986 issue of *AJNR* and the January 1987 issue of *AJR*.

Received March 31, 1986; accepted after revision May 28, 1986.

Presented at the annual meeting of the American Society of Neuroradiology, San Diego, January 1986.

¹ All authors: Department of Radiology, University of California, San Francisco, CA 94143. Address reprint requests to W. L. Olsen, San Francisco General Hospital, San Francisco, CA 94110.

AJNR 7:1039-1042, November/December 1986
 0195-6108/86/0706-1039

© American Society of Neuroradiology

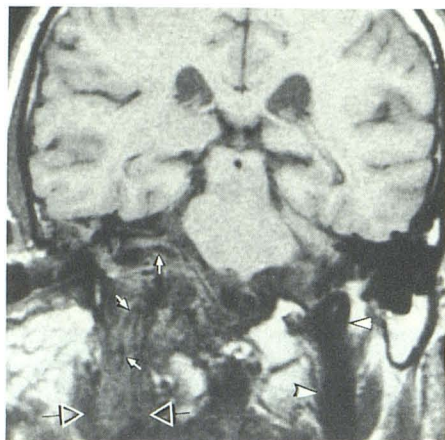
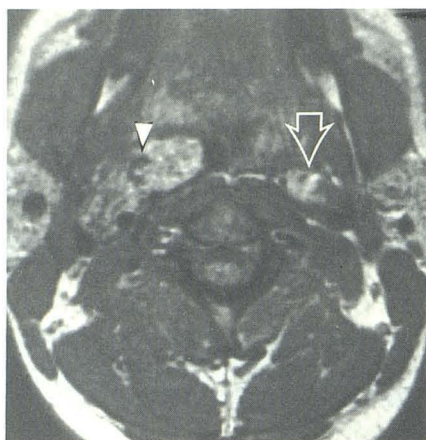
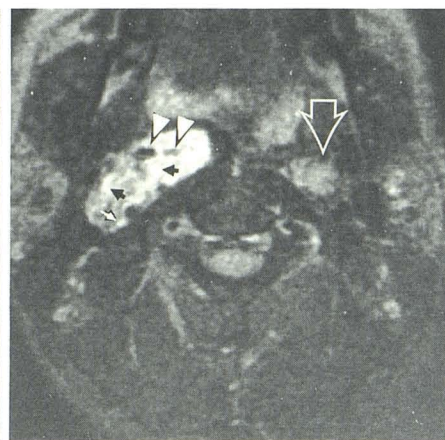


Fig. 1.—Right jugulotympanic paraganglioma. TR 600 msec, TE 25 msec, 1.5 T. Coronal section shows serpiginous areas of signal void reflecting hypervascularity typical of paragangliomas (solid arrows). Tumor extends intracranially and down lumen of right internal jugular vein (open arrows). Normal left internal jugular vein has signal void characteristic of blood flow (arrowheads). (Courtesy of Bent Kjos.)



A



B

Fig. 2.—Bilateral carotid body paragangliomas. A, TR 2000 msec, TE 40 msec, 1.5 T. B, TR 2000 msec, TE 80 msec, 1.5 T. Even-echo rephasing phenomena characteristic of slow blood flow are suggested by punctate areas of high signal intensity that have increased markedly between first- and second-echo images (solid arrows). Punctate areas of signal loss reflect regions of high-blood-flow velocity (arrowheads). Small left carotid body tumor (open arrows).

small separate glomus tympanicum tumor. In total, there were seven carotid body tumors, six jugulotympanic tumors, one vagal paraganglioma, and one glomus tympanicum tumor. Selective angiography was performed in all patients. Contrast-enhanced CT using a rapid drip infusion was performed in eight patients. Pathology was available in seven patients. In the other three patients, the clinical features and radiographic appearance were considered to be typical of paragangliomas. They were treated with radiation therapy without histologic confirmation.

MR examinations were performed with a 0.35 T unit (Diasonics MT/S) in six patients (nine tumors) and with a 1.5 T unit (GE Signa) in four patients (six tumors). Multisection, spin-echo (SE) T1- and T2-weighted images were obtained. MR imaging parameters were repetition time (TR) 500–600 msec, echo time (TE) 25–40 msec (T1-weighted) and TR 1500–2000 msec, TE 25–80 msec (T2-weighted). T2-weighted images were obtained using a multiecho SE technique. In almost all cases, section thickness was 5 mm with an acquisition matrix of 256×256 . There were no interslice gaps with the Diasonics images. On the GE studies, a 20% gap was used with T1-weighted images and a 50% gap was used with T2-weighted images. CT scans were obtained on either a GE 8800 or 9800 scanner.

Results

Thirteen paragangliomas in eight patients were detected by CT and MR. In two other patients imaged with MR alone, two paragangliomas were seen. A small glomus tympanicum tumor, well visualized by angiography and CT, was less conspicuous on MR because of partial-volume averaging with adjacent middle ear inflammation. It was seen only in retrospect. This patient also had bilateral carotid body tumors.

In 12 of the 15 tumors, there were multiple punctate and serpiginous areas of signal void due to high-velocity flow in tumor vessels seen on both T1- and T2-weighted images

(Figs. 1 and 2). In three patients the tumors demonstrated foci of even-echo rephasing indicating relatively slow blood flow (Fig. 2). These even-echo rephasing phenomena appeared on T2-weighted images as punctate areas of increased signal intensity on the second echo, particularly in regions where there was little or no signal present on the first echo [4, 5]. Three tumors demonstrated neither high-velocity signal loss nor even-echo rephasing phenomena. Two of these lesions were less than 2 cm in maximum dimension (Fig. 3). The third lesion was studied by MR after angiographic embolization.

The relation of the paraganglioma to the adjacent carotid artery and/or jugular vein was well demonstrated by MR in all cases (Fig. 4). Focal obliteration and invasion of the jugular vein was demonstrated by MR in six cases and was confirmed by angiography (Figs. 1 and 3). CT scans were available in four of these cases. Since both tumor and vein enhanced, invasion was seen less easily on CT than on MR.

The T1 and T2 characteristics of the paragangliomas showed regional variation when compared visually with nearby muscle or brain. In general, the tumors exhibited relatively prolonged T1 and T2 relaxation times. On T1-weighted images (TR \leq 600 msec, TE \leq 40 msec), 11 tumors were of approximately equal signal intensity to adjacent muscle, while four tumors were slightly higher in intensity than surrounding muscle (Fig. 1). On T2-weighted images (TR \geq 1500 sec, TE \geq 56 msec), all tumors showed a variable but greater signal intensity than muscle (Fig. 2). The appearance of high-signal and low-signal regions resulted in a "salt-and-pepper" heterogeneity on T2-weighted images that has not been seen by us in any other mass lesion imaged with MR. T2-weighted images were better for identifying the two small lesions. T1-weighted images gave the better spatial resolution

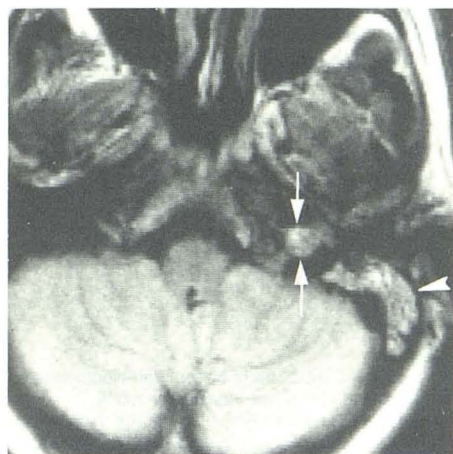
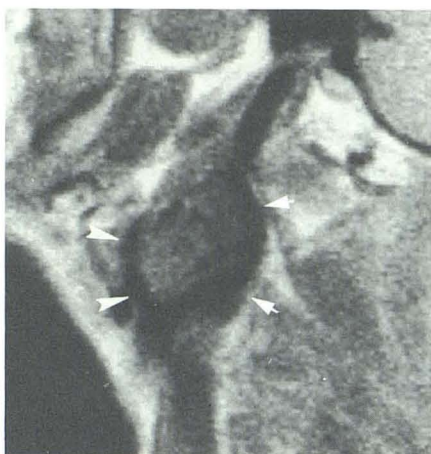
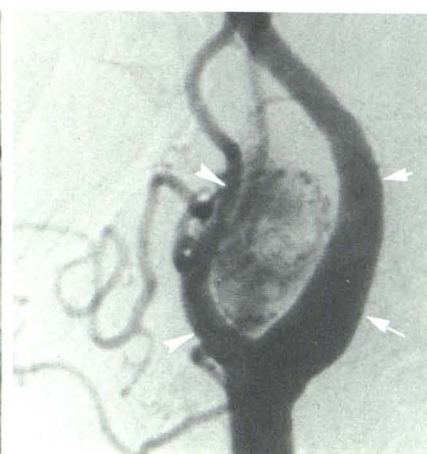


Fig. 3.—Left jugular bulb paraganglioma. TR 2000 msec, TE 35 msec, 0.35 T. Small mass within jugular bulb (*arrows*) does not show evidence of hypervascularity characteristic of larger paragangliomas. Mastoid air cell signal (*arrowhead*) secondary to obstruction of eustachian tube.

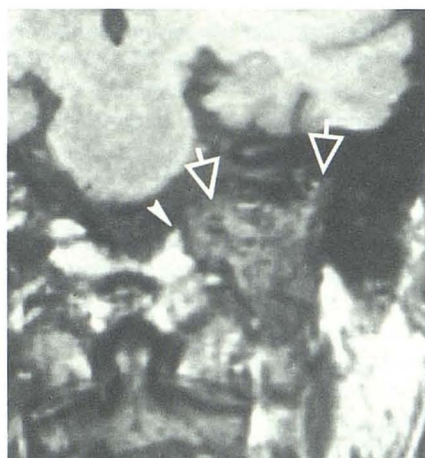


A



B

Fig. 4.—Carotid body paraganglioma. **A**, TR 500 msec, TE 30 msec, 0.35 T. **B**, Lateral common carotid arteriogram. Posterior displacement of internal carotid artery (*arrows*) and anterior displacement of external carotid artery (*arrowheads*) are well demonstrated by both studies. MR image was obtained using a 128×256 image matrix, accounting for less than optimal spatial resolution.



A



B

Fig. 5.—Jugulotympanic paraganglioma. **A**, TR 600 msec, TE 25 msec, 1.5 T. **B**, Coronal CT section using prospective bone review algorithm. Bony detail of destructive process at skull base is optimally demonstrated by CT (*solid arrows*). Invasion of jugular tubercle is also shown by MR (*arrowhead*), as is intracranial extent of tumor and its relation to brainstem (*open arrows*).

of the internal matrix of the paragangliomas. T1-weighted images in the coronal and sagittal planes were best for judging the relation of the tumor to nearby vessels and intracranial contents.

Skull-base erosion was present in all six jugulotympanic tumors (Figs. 1 and 5). MR and CT demonstrated the skull-base erosion in each case. Subtle areas of bone destruction were more easily identified on CT. The relation of the tumor to intracranial structures was better seen on MR. Coronal images were optimal for demonstrating skull-base destruction and intracranial extension (Figs. 1 and 5). Unilateral denervation atrophy of the tongue caused by hypoglossal nerve damage was present in two patients. The atrophy was more striking on MR than on CT because of the greater signal contrast between fat and muscle, especially on T1-weighted images.

Discussion

MR imaging provides a unique tool to assess the patient with suspected paragangliomas. MR detects the vascular nature of these lesions, and in our experience is highly characteristic for the diagnosis of paraganglioma. Indeed, in 12 of our 15 cases, multiple areas of low signal resulting from high-velocity signal loss characteristic of rapid arterial and venous blood flow were present in the matrix of these tumors on both T1- and T2-weighted images. In our experience, other tumors involving the carotid space and skull base—such as neurofibromas, schwannomas, and nasopharyngeal malignancies—have a less vascular appearance to their internal matrix (Fig. 6). This appearance was also noted with very small paragangliomas (Fig. 3). Calcification can also produce signal void on MR images; however, serpiginous calcification

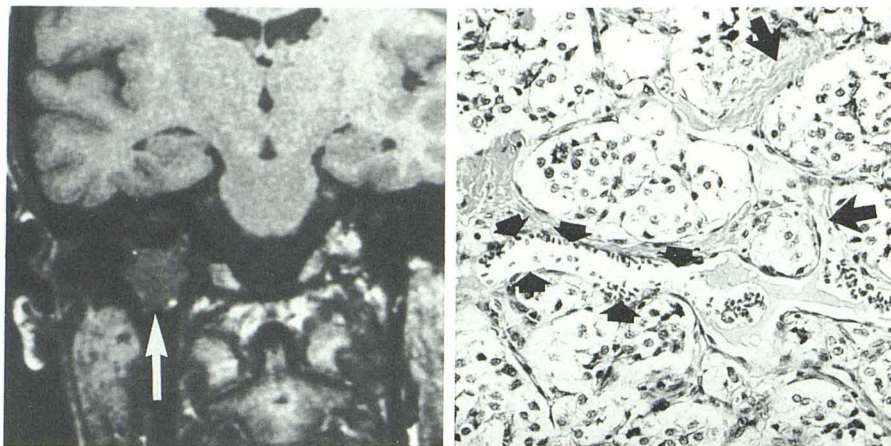


Fig. 6.—Schwannoma of vagus nerve in jugular foramen (proven). TR 600 msec, TE 25 msec, 1.5 T. Homogeneous signal intensity of mass in jugular foramen (arrow).

Fig. 7.—Carotid body tumor. Pathologic slide, H and E stain. Prominent vascular channels (small arrows) and lobules of cells separated by thick fibrous septae (large arrows) are typical of paragangliomas.

in neck masses is rare and was not a feature in any of our CT studies.

Paragangliomas in the head and neck occur most often in the carotid body and have a multicentric origin in about 3% of all patients, increasing to 26% in patients with familial tendencies [6]. Pathologically, the paragangliomas are composed of nests of cells separated by numerous vascular channels in a fibrous matrix (Fig. 7). In the past, angiography has been the primary radiographic tool in the preoperative assessment of head and neck paragangliomas. Angiography demonstrates the vascular supply and pattern of these lesions as well as the extent of the tumor and its relation to the carotid artery and internal jugular vein (Fig. 4A). Angiography also detects occlusion of the internal jugular vein, a common finding with larger lesions. Bilateral carotid arteriography is helpful in assessing the rare bilateral lesion. CT demonstrates the extent of these lesions, including skull-base and intracranial invasion [7, 8]. The vascularity of paragangliomas is reflected by their intense enhancement on CT. However, since other tumors, most notably schwannomas, also enhance on CT after drip infusion of contrast material, the profusely vascular nature of paragangliomas is not reliably detected without bolus-enhanced dynamic CT [1–3].

The advantages of MR over CT include the ability to characterize the vascularity of a lesion without the use of intravenous contrast material as well as demonstration of the tumor extension into the posterior fossa without the high-spatial-frequency artifact from the petrous bone that frequently diminishes the quality of CT examination. Additional information regarding the relation of the tumor to the surrounding important vascular structures such as the carotid artery and jugular vein was also more easily evaluated by MR than CT (Figs. 1–4). We recommend obtaining both T1- and T2-weighted images. T1-weighted images give better spatial resolution and better show the highly vascular internal matrix of the tumor. T2-weighted images give better tissue contrast, making smaller lesions more conspicuous. In larger lesions, the "salt-and-pepper" appearance on T2-weighted images was characteristic of paragangliomas. T1-weighted coronal images are best for evaluating intracranial extension.

MR certainly has limitations, as evidenced by the single lesion that was less conspicuous on MR because of its small size and apparent partial-volume averaging. Thin sections displayed on a 256×256 matrix will optimize detection of these smaller lesions and in our experience are necessary imaging parameters. The ability to detect the relation of the tumor to the important structures of the middle ear, such as the ossicles and the semicircular canals, is better with CT than MR.

In conclusion, angiography will still be necessary to outline the vascular supply of these lesions before surgical resection and for embolization therapy. However, MR can identify large paragangliomas with great specificity, obviating angiography before radiation therapy. Fine-needle aspiration biopsy techniques may be performed once MR has characterized the lesion as a paraganglioma.

REFERENCES

1. Shugar MA, Mafee MF. Diagnosis of carotid body tumors by dynamic computed tomography. *Head Neck Surg* 1982;4:518–521
2. Mafee MF. Dynamic CT and its application to otolaryngology—head and neck surgery. *J Otolaryngol* 1982;11:307–318
3. Som PM, Biller HF, Lawson W, Sacher M, Lanzieri CF. Parapharyngeal space masses: an updated protocol based upon 104 cases. *Radiology* 1984;153:149–156
4. Waluch V, Bradley WG. NMR even echo rephasing in slow laminar flow. *J Comput Assist Tomogr* 1984;8:594–598
5. Bradley WG, Waluch V. Blood flow: magnetic resonance imaging. *Radiology* 1985;154:443–450
6. Batsakis JG. *Tumors of the head and neck: clinical and pathological considerations*. Baltimore: Williams & Wilkins, 1979:369–379
7. Duncan AW, Lade EE, Deck MF. Radiologic evaluation of paragangliomas of the head and neck. *Radiology* 1979;132:99–105
8. Som PM, Biller HF, Lawson W. Tumors of the parapharyngeal space: preoperative evaluation, diagnosis and surgical approaches. *Ann Otolaryngol [Suppl]* 1981;90:3–15